NJC

New Journal of Chemistry

A journal for new directions in chemistry

Accepted Manuscript

This article can be cited before page numbers have been issued, to do this please use: F. Isaia, A. Garau, M. C. Aragoni, M. Arca, C. Caltagirone, F. Demartin, V. Lippolis and T. Pivetta, *New J. Chem.*, 2022, DOI: 10.1039/D2NJ00526C.

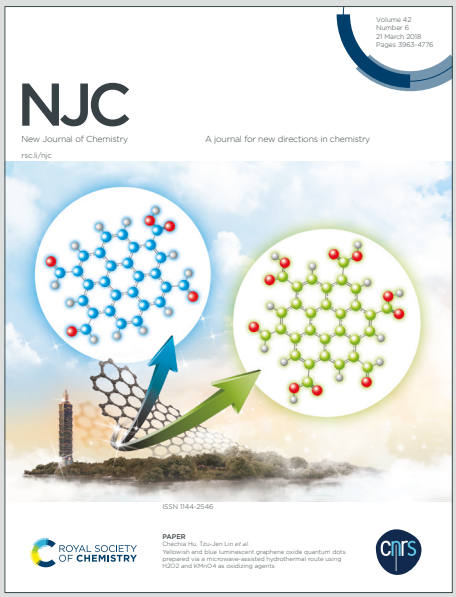

View Article Online
DOI: 10.1039/D2NJ00526C

A new assembly of diiodine molecules at 1,3-Dimethylimidazole-2-thione (Me_2ImS) template: Crystal Structure of $(Me_2ImS)_2\cdot(I_2)_5$

Alessandra Garau,[a] M. Carla Aragoni,[a] Massimiliano Arca,[a] Claudia Caltagirone[a] Francesco Demartin,[b] Francesco Isaia,[a,*] Vito Lippolis,[a] Tiziana Pivetta[a]

[a] Dipartimento di Scienze Chimiche e Geologiche, Università degli Studi di Cagliari, Cittadella Universitaria, 09042 Monserrato (CA), Italy. Tel: +39 070 67544. E-mail: isaia@unica.it

[b] Dipartimento di Chimica, Università degli Studi di Milano, via Golgi 19, 20133 Milano. Italy.

Abstract

The new poly(I_2) adduct $[(Me_2ImS)_2\cdot(I_2)_5]$ (Me_2ImS = 1,3-dimethylimidazole-2-thione) has been synthesized and characterized by single crystal X-ray diffraction analysis. Units of $[(Me_2ImS)_2\cdot(I_2)_5]$ are located about a crystallographic inversion center, in which five diiodine molecules display interatomic contacts in a "head-to-tail" sequence given a $-(I_2)_5-$ chain interacting at each end with one Me_2ImS molecule, CCDC 2133501. The *S*-bonding of Me_2ImS to I_2 is described as donor-acceptor interaction in which I_2 acts as acceptor through the σ*(I-I) orbital resulting in an electronic charge transfer from the thioamide moiety. The bond distances *d*(S-I(1)) (2.504(2) Å) and *d*(I(1)-I(2)) (3.133(1) Å) are indicative of a strong interaction. Based on the S-I, I-I bond distances, the calculated values of the electronic charge densities, and the Raman spectroscopy data it is reasonable to represent the compound as an extended polarised system: $[(Me_2ImS)\text{-}I(1)]^{\delta+}\cdots I(2)^{\delta-}\cdots I(3)\text{-}I(4)^{\delta-}\cdots(I(5)\text{-}I(5)^{a})\cdots I^{\delta-}\text{-}I\cdots I^{\delta-}\cdots[I\text{-}(Me_2ImS)]^{\delta+}$. The molecular electrostatic potential maps of the three adducts $Me_2ImS\cdot I_2$, $Me_2ImS\cdot I_2\cdot I_2$, and $MeImHS\cdot I_2$ (MeImHS = methimazole) have been reported to clearly identify the areas of charge increment (electron belt) and depletion (σ-hole), thus the directionality of noncovalent interactions.

Introduction

Neutral Charge Transfer (C.T.)-complexes between diiodine (I_2) and molecules containing sulfur donor atoms (DS) represent an important and extensively investigated class of compounds formally featuring a roughly linear S···I-I bond.[1] C.T.-complexes still attract a lot of interest in many fields of chemistry including crystal engineering, metal recovery processes from waste electrical and electronic equipment (WEEE),[2-11] and pharmacology for their involvement in the mechanism of action of anti-thyroid drugs.[12] The apparently simple reaction between small molecules containing the thioamide group and I_2 reveals that the nature of the products obtained is notably influenced by both the intrinsic nature of DS, and the reaction condition (in particular: the polarity of the solvent and the reagents molar ratio). The main classes of compounds identified in the solid state are shown in Scheme 1.

View Article Online
DOI: 10.1039/D2NJ00526C

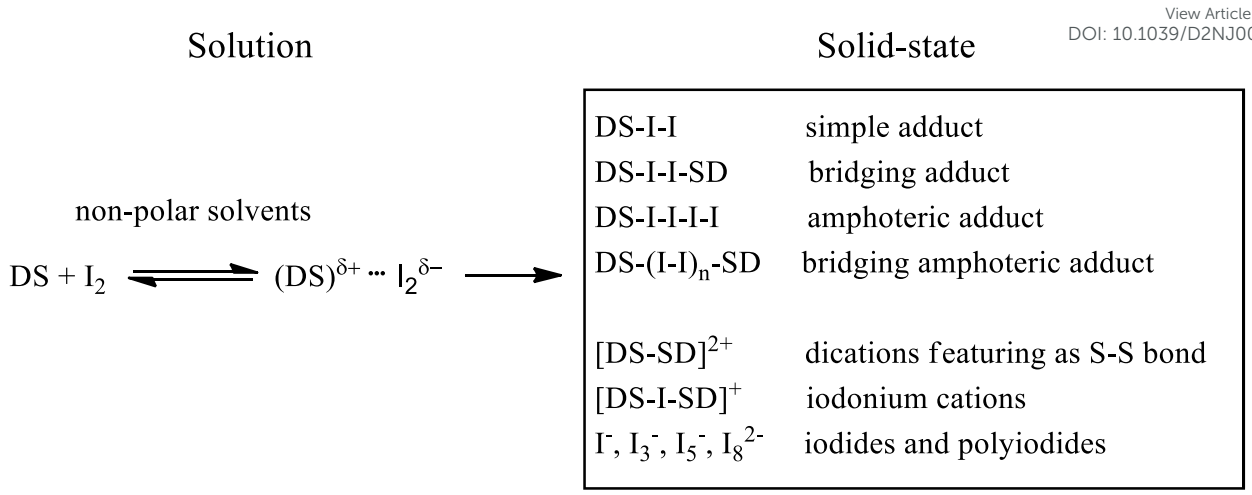

Scheme 1. Schematic representation of the compounds obtainable from the reaction of a *S*-donor Lewis base (DS) and I_2. This scheme aims to illustrate the various classes of compounds obtainable without any implication on the nature of the chemical bond involved.

In non-polar solvents, reactions between DS and I_2 generally yield only 1:1 C.T. complexes with formation constant K_f depending on the equilibrium molar concentrations according to the equation $K_f = [DS{\cdot}I_2]/[DS][I_2]$.[13] The interaction arises as a result of electronic density donation from a lone pair (LP) of electrons localized on the sulphur atom to the σ* antibonding lowest unoccupied molecular orbital (LUMO) of the I_2 molecule. Depending on the charge density transferred by DS to I_2 and the nature of the solvent, this can result in lengthening of the I–I bond up to the breaking of this bond and formation of new species.[14]

The principal structural types of reported solid C.T.-complexes can be classified into four main groups depending on their structural features and stoichiometries. They can be *simple* (DS-I-I) or *bridging complexes* (DS-I-I-SD), in both cases the thioamide sulphur atom/s interacts with I_2 *via* halogen bond/s forming species with 1:1 or 2:1 DS to I_2 molecular stoichiometry. If the DS⋯I_2 interaction is strong enough to result in a strong polarization of the interacting iodine molecule [$(DS\text{-}I)^{\delta+}\cdots I^{\delta-}$], the terminal iodine can act itself as a donor species due to the acquired significant negative charge density with formation of diiodine rich systems defined as *amphoteric* adducts [DS-I-I-$(I\text{-}I)_n$] or *bridging amphoteric* complexes [DS-$(I\text{-}I)_n$-SD] featuring different distributions of iodine-iodine and sulphur-iodine bond lengths.[2,15,16] An example of the variety of compounds that can be obtained even from the same donor molecule, is provided by the thioamide methimazole (Fig. 1). Through the reaction with diiodine we separated the novel oxidation products methimazole dication-disulfide octaiodide $[(MeImHS\text{-})_2]I_8$, dimer monocation methimazole-disulfide triiodide-pentaiodide $[2(MeImHS\text{-}SImMe)]I_3I_5$,[17] and the 1:1 adduct $MeImHS{\cdot}I_2$.[18]

Based on these considerations and pursuing our interest in studying the reaction between diiodine and molecules structurally related to methimazole, we have investigated the reaction of iodine with 1,3-

dimethyl-imidazole-2-thione (Me_2ImS) (Fig. 1). On this matter, Suszka (1985)[13a] studied the equilibrium reaction $Me_2ImS + I_2 = Me_2ImS{\cdot}I_2$ determining the value of the formation constant (K_f) of the 1:1 C.T.-complex $Me_2ImS{\cdot}I_2$ (CH_2Cl_2, 25°C) which turned out to be K_f =106905 ± 510 L mol^{-1}; while Freeman (1988) reported both on the crystal structure of the 1:1 C.T.-complex $Me_2ImS{\cdot}I_2$ (in two crystalline forms, α and β),[19] and on the spectroscopic characterisation of the iodonium complex bis(1,3-dimethyl-imidazole-2-thione)iodine(I) iodide $[(Me_2ImS)_2I]I$; these compounds were obtained from the reaction of Me_2ImS and I_2 in CH_2Cl_2 using 1:1 and 2:1 reaction molar ratios, respectively. Since it appears that the stoichiometry of the compounds obtained by Freeman reflects the molar ratio of the reagents used in the reactions, we examined different Me_2ImS:I_2 molar ratios with the aim of finding out whether further structural motifs could be found for such a system.

In this paper, we report the synthesis, and the X-ray crystal structure of the obtained poly(I_2) adduct $[(Me_2ImS)_2{\cdot}(I_2)_5]$ (**1**) and a comparison of the structural data with those of two related adducts reported in the literature $Me_2ImS{\cdot}I_2$ and $MeImHS{\cdot}I_2$ (Fig 1). Theoretical calculations at DFT level by using the ωB97XD functional and the 6-31G* basis set are also performed. Finally, some hypotheses on the antithyroid behavior of Me_2ImS compared to that of methimazole are reported.

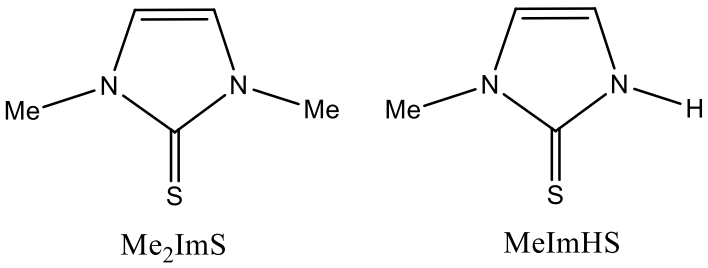

Fig. 1 Formula schemes of 1,3-dimethyl-imidazole-2-thione (Me_2ImS) and 1-methyl-3*H*-imidazole-2-thione, methimazole (MeImHS) considered in this paper.

Results and Discussion.

The synthesis of $[(Me_2ImS)_2{\cdot}(I_2)_5]$ was carried out in a two-step process. The first one involved the preparation in CH_2Cl_2 of the 1:1 C.T. complex $Me_2ImS{\cdot}I_2$ (T = 10 °C) by reacting equimolecular amounts of Me_2ImS and I_2. Compared to the synthesis procedure reported by Freeman,[19] the following changes were carried out to limit the formation of oily by-products: i) use of more diluted reagent solutions, from 0.02 mmol/mL to 0.0078 mmol/mL, respectively, ii) reduction of the reaction temperature (from r. t. to 10 °C), and lastly iii) conducting the reaction by mixing small volumes of I_2 and Me_2ImS solutions simultaneously to achieve a molar ratio between the two species close to 1:1 throughout the reaction. In the second step of the synthesis, another equivalent of a refrigerated I_2 solution was slowly added (CH_2Cl_2, T = 10°C) to the clear dark-red solution obtained in the first step,

by slow evaporation of the solvent, dark-red crystals having the unusual $Me_2ImS:I_2$ stoichiometry ratio of 1:2.5 were separated from the solution. A single crystal XRD analysis revealed the formation of the molecular compound $[(Me_2ImS)_2\cdot(I_2)_5]$ (**1**). Crystal data and structure refinement details are summarized in ESI-Table S1, selected interatomic distances and angles are reported in ESI-Table S2. The UV-Vis spectrum of compound **1**, dissolved in CH_2Cl_2 and recorded in the range 250-550 nm (Fig. S1 in the ESI), shows an intense band (charge-transfer transition) at λ_{CT} = 350 nm (ε_{CT} = 30360 L mol^{-1} cm^{-1}). The shape of the band, the values of λ_{CT} and ε_{CT} are essentially coincident with those reported by Suszka for the $Me_2ImS\cdot I_2$ adduct (λ_{CT} = 349.7 nm (ε_{CT} = 30100 L mol^{-1} cm^{-1}).[13a] The absence in the spectrum of any band at *ca*. 290 nm excludes the presence of triiodide ions.[13a] These data suggest that compound **1** is formed by addition of iodine molecules to the $Me_2ImS\cdot I_2$ adduct in the process of solution concentration by evaporation of the solvent.

Several reaction attempts using the two-step procedure described above and a $Me_2ImS:I_2$ molar ratio of 1:3 only led to the formation of oily products and/or lacquers during the addition of the third equivalent of I_2 to the solution.

Crystal Structure of $[(Me_2ImS)_2\cdot(I_2)_5]$ (1) and Theoretical Calculations

Crystals of compound **1** contain units of $[(Me_2ImS)_2\cdot(I_2)_5]$ located about a crystallographic inversion center, in which five diiodine molecules interact in a "head-to-tail" sequence to give a $-(I_2)_5-$ chain interacting at each end with one Me_2ImS molecule (Fig. 2). Analysis of the X-ray crystal structure of **1** highlights the mutual effects the *S*-donor Me_2ImS units exert on the I_2 molecules and *vice versa*.

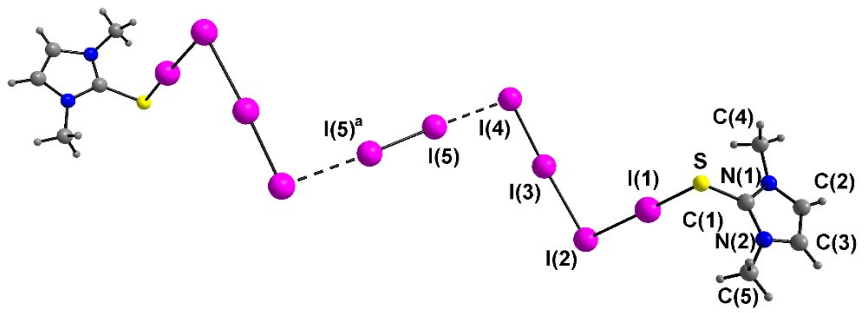

Fig. 2 The view of the centrosymmetric $[(Me_2ImS)_2\cdot(I_2)_5]$ unit in **1** with the labelling scheme adopted. The crystallographic inversion center is located at the midpoint of the I(5)-I(5)ª bond. N(1)-C(1) 1.320(9), N(2)-C(1) 1.343(8), C(1)-S 1.732(7), S-I(1) 2.504(2), I(1)-I(2) 3.133(1), I(2)-I(3) 3.076(1), I(3)-I(4) 2.801(1), I(4)-I(5) 3.447(1), I(5)-I(5)ª 2.748(1) Å; C(1)-S-I(1) 100.1(2), S-I(1)-I(2) 177.43(5), I(1)-I(2)-I(3) 91.14(2), I(2)-I(3)-I(4) 177.05(2), I(3)-I(4)-I(5) 92.3(2)°, torsion angle around C=S: N1-C1-S-I1 97.7(6) °. Symmetry operation ª = - x, -y-1, -z. ORTEP plot in ESI-Figure S2.

As a result of the donor-acceptor interaction ($Me_2ImS\rightarrow I_2$)[20] the formation of the S-I(1) bond whose length (2.504 Å) is significantly shorter of the sum of the relevant van der Waals radii of the interacting

atoms (Σr_{vdw}(S,I) = 3.78 Å)[21] is observed. Conversely, the I(1)-I(2) bond (3.133 Å) results in a marked elongation compared to that observed in crystalline I_2 (2.715 Å at 110 K)[22] with consequent lowering of the I-I bond order (n), (n = 0.28 and 0.85 in **1** and I_2(s), respectively).[23] Another consequence of the donor-acceptor interaction is the elongation of the C(1)-S bond from 1.695 Å in Me_2ImS to 1.732 Å,[19] indicating a reduction of the C=S double-bond character. [Average bond length for C=S and C-S: 1.67(2) Å and 1.77(2) Å, respectively].[24]

The sulphur atom binds the I(1)-I(2) molecule to give a linear S-I-I arrangement (S-I-I angle of 177.43(5)°) with the I-I molecule lying quasi-perpendicular to the NCS plane with the torsion angle N-C-S-I around C-S of 97.0°. Such a "perpendicular" arrangement of the I(1)-I(2) iodine atoms on the less sterically crowded side of the Me_2ImS moiety eschews the steric interaction with the methyl groups located in the plane of the pentatomic ring.[13b] In C.T. thione/thioamide-I_2 adducts having a S-I-I arrangement a direct relationship exists between the *d*(I-I) and *d*(S-I) bond distances from which the nature of the donor-acceptor interaction (very strong, strong, or weak) can be classified.[13c,25] In **1** the values of *d*(S-I(1)) (2.504(2) Å) and *d*(I(1)-I(2)) (3.133(1) Å) fit very well into the correlation curve in the strong interaction region (Fig. S3 in the ESI), this fact strongly support a description of a polarized system as $[>C\text{-}S\text{-}I]^{\delta+}\cdots I^{\delta-}$.

Theoretical calculations at the equilibrium geometry, atomic charges and molecular electrostatic potential (MEP) maps were performed at the DFT level as useful descriptors for the reactivity of the studied molecules. Calculations were performed on the fragment $Me_2ImS\cdot I_2\cdot I_2$ of **1**, and on the related adducts $Me_2ImS\cdot I_2(\alpha)$ and $MeImHS\cdot I_2$. Natural charges calculated at the experimental structural geometry Table 1, (Table S3 in the ESI) show that the net charge transferred from the donors Me_2ImS and MeImHS to the bound diiodine/s system is similar in compounds $Me_2ImS\cdot I_2\cdot I_2$ and $Me_2ImS\cdot I_2$ (+0.372 |e| and +0.364 |e|, respectively) but significantly smaller in $MeImHS\cdot I_2$ (+0.216 |e|) for the lower inductive effect due to the presence of only one *N*-methyl group. The calculated charges relative to the S-I-I segment in 1:1 adducts $Me_2ImS\cdot I_2$ (α crystalline form)[19] (ESI-Table S4) and $MeImHS\cdot I_2$ (ESI-Table S5) indicate that the charge transferred is largely located on the terminal I(2) iodine atom with the I(1) iodine becoming nearly neutral. Of interest is the charge separation created between I(2) and I(1), +0.418 |e| and +0.202 |e|, respectively, that radically changes iodine atoms' reactivity of the I_2-adducts when compared to that of molecular I_2. [1,10,11] In the $Me_2ImS\cdot I_2\cdot I_2$ system the natural charge calculated on the iodine fragment I(1)-I(2)-I(3)-I(4) is -0.372 |e|, with the iodine atoms I(1) and I(3) becoming nearly neutral (+0.018 e and +0.008 e, respectively) and the iodine atoms I(2) and I(4) having a negative charge of -0.243 |e| and -0.155 |e|, respectively. It is well recognised in the literature that iodine atoms involved in the R-I_b-I_t system (R= halogen, C, N, S…; I_b = bridging iodine; I_t = terminal iodine) can give rise to donor-acceptor interactions. Both iodine I_b, and iodine I_t could act as donors using *p*-electron LPs, and iodine I_t could also act as acceptor through the σ^* orbital of the I-I bond at its

apical position.[13b,26] Thus in compound **1**, the I(1)-I(2) moiety acts simultaneously as electron acceptor when interacting along its molecular axis S→I(1)-I(2), [S-I-I angle of 177.43(5)°] and as electron donor when interacting perpendicular to it I(1)-I(2)→I(3)-I(4) [I(1)-I(2)-I(3) angle of 91.14(2)°]. In the latter case the interaction derives from electron donation by a *p*-type lone pair to the antibonding I(3)-I(4) σ* orbital.[13b,26] Consequently, the bond distance I(3)-I(4) of 2.801(1) Å is 0.086 Å longer than in I_2(s), and the linear asymmetric system $I(2)^{\delta-}\cdots I(3)\text{-}I(4)^{\delta-}$ features an angle of 177.05(2)° with a bond distance I(2)···I(3) of 3.076(1) Å.

The weak interaction of I(4)/I(4)[a] on the I(5)/I(5)[a] molecule, that occupies the inversion centre, is mutually exclusive leaving the bridging molecule only slightly perturbed with a bonding distance of 2.748 Å and the I(4)/I(4)[a]···I(5)/I(5)[a] contacts (3.447 Å) comparable to those found in I_2(s) of 3.50 Å.[22] Given the paucity of structurally characterised poly(I_2) containing-compounds such as **1**, we thought it would be of interest to record the Raman spectrum of compound **1** to further characterise it. Solid state I_2 shows a single Raman band at 180 cm^{-1}, symmetric stretching mode ν_1(I-I).[27a] This is expected to move to lower wavenumbers (typically in the range 180-140 cm^{-1}) upon coordination to a *S*-donor species. In the case of weak or medium-weak adducts (d(I-I) < 2.86 Å) the ν(I-I) Raman frequencies can be correlated to the d(I-I) bond distances.[27b]

The Raman spectrum of compound **1** (Fig. S4 in the ESI) recorded in the region 50-500 cm^{-1} shows intense bands at 148 and 172 cm^{-1}, which can be attributed to the ν(I-I) stretching vibration of the slightly perturbed diiodine molecules I(3)-I(4) and I(5)-I(5)[a], in agreement with the relevant bond lengths of 2.801 and 2.748 Å, respectively.

On these grounds it is reasonable to describe the fragment $Me_2ImS\cdot I_2\cdot I_2$ in **1** as an extended polarised system with a positive charge δ^+ associated to the whole Me_2ImS donor, and the I(2) and I(4) atom carrying the negative charge δ^-, i.e. $[(Me_2ImS)\text{-}I]^{\delta+}\cdots I^{\delta-}\cdots I\text{-}I^{\delta-}$.

Table 1. Selected bond distances (Å), calculated natural charges (|e|) for fragment $[(Me_2ImS)\cdot(I_2)\cdot(I_2)]$ of compound **1**, $Me_2ImS\cdot I_2(\alpha)$ and $MeImHS\cdot I_2$.

Compound	*d*(S-I(1))	*d*(I(1)-I(2))	C(1)	S	I(1)	I(2)	I(3)	I(4)
$[(Me_2ImS)_2\cdot(I_2)\cdot(I_2)]$ in **1**	2.504	3.133	+0.269	-0.173	+0.018	-0.243	+0.008	-0.155
$Me_2ImS\cdot I_2$[a]	2.616	2.967	+0.316	-0.122	+0.027	-0.391		
$MeImHS\cdot I_2$[b]	2.593	2.991	+0.264	-0.208	-0.007	-0.209		

[a] Bond distances of the α crystalline form reported in ref. 19; [b] Bond distances taken from ref. 18.

Crystal Packing. Additional I(4)…I(4) interactions of 3.707(1) Å between adjacent $[(Me_2ImS)_2\cdot(I_2)_5]$ units give rise to an "herring-bone" polymeric assembly of diiodine molecules as shown in Fig. 3. Some larger I···I interactions, but below the sum of the relevant van der Waals radii (Σr_{vdw}(I,I) = 4.34 Å),[21a] are also reported in the ESI, Table S2.

View Article Online
DOI: 10.1039/D2NJ00526C

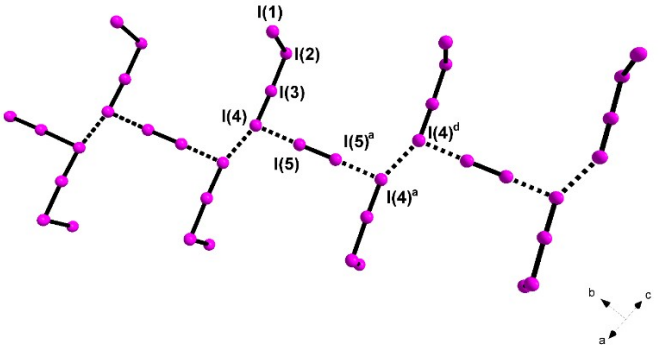

Fig. 3 Partial view of the poly(I_2) assembly in [($Me_2ImS)_2\cdot(I_2)_5$] (**1**). Me_2ImS donor units are omitted for clarity.

The $(Me_2ImS)_2\cdot(I_2)_5$ units are packed in the crystal aligned along the [100] direction and form kinked layers stacked along [001] (Fig. 4). With the exception of I(1) and its centrosymmetric counterpart, the remaining iodine atoms system of each unit is planar and the 1,3-dimethyl-imidazole-2-thione molecule is oriented almost parallel to the plane defined by these atoms. Considering the value of 3.37 Å as an upper limit for the sum of the van der Waals radii of iodine and hydrogen,[21b] in the crystal packing only five interactions of the thioamide methyl hydrogens with the iodine atoms (3.19-3.37 Å) shorter than the sum of the relevant van der Waals radii are present.

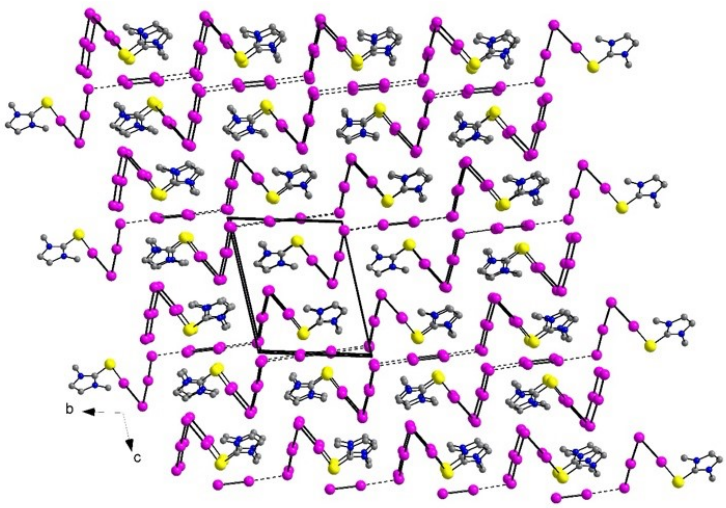

Fig. 4. Projection of the crystal packing along the [100] direction.

The compound here discussed, $(Me_2ImS)_2(I_2)_5$, represents, therefore, a rare example of a neutral extended poly(I_2) arrangement held up by soft-soft $I_2\cdots I_2$ interaction at the Me_2ImS template. In fact, despite the numerous examples of polyiodide anions and cations which demonstrate the high catenating ability of diiodine to assemble in a wide range of structural motifs, extended neutral poly(I_2) arrangements are extremely rare and the best example so far reported is I_2 itself. Several I_2 adducts with a diiodine content higher than the 1:1 stoichiometry normally feature only discrete $D\cdot I_2\cdots(I_2)_n$ or

D·I_2···$(I_2)_n$···I_2·D arrangements, while extended neutral networks of diiodine molecules have been described for the adducts TPPS·3I_2 (triphenylphosphine sulfide)[5b] and mbtse·2I_2 (*N*-methylbenzothiazole-2(3H)-selone)[5c]. We can reasonably hypothesise that the methylation of both nitrogen atoms in Me_2ImS increases the negative charge on the sulphur atom resulting in a greater donor ability of the molecule as compared to MeImHS. As a consequence, the tendency of coordinated diiodine to further interact with I_2 and form catenated species is promoted. Accordingly, the few cases of imidazole-2-thione I_2-adducts showing iodine-iodine catenation all display substituents on both *N*-endocyclic atoms[28] whilst mono-methyl substituted imidazole only form 1:1 I_2-adducts.

Molecular electrostatic potential (MEP) maps

The molecular electrostatic potential (MEP) map is a useful descriptor for determining molecules' reactive behaviour, especially in noncovalent interactions.[29] The electrostatic potential $V(\mathbf{r})$ is a physical observable that can be determined computationally.[29b] The MEP surface of an outer region of a molecule indicates areas of electron excess and deficiency. The values of the electrostatic potential (kJ/mol), calculated at the DFT level at the structural experimental geometry, are represented by different colours: the red colour indicates the region with the most negative potential whereas the blue colour indicates the most positive region.

The MEP maps of the Me_2ImS moiety in Me_2ImS·I_2·I_2 (Fig. 5, and Fig S5 in ESI) and in Me_2ImS·I_2(α) (Fig. 6) show significant amounts of electron-deficient sites (blue) overlapping the N-CH-CH-N hydrogens, and only a slight electron-deficient site (light blue) over the NCH_3 hydrogens due to the electronegative nitrogen atoms binding the methyl groups. These hydrogen atoms are reasonably suitable for the formation of noncovalent interactions with electron-rich sites as it is found in the crystal-packing of the compound Me_2ImS·I_2(α) where I···HC interactions between adjacent molecules in the range of 3.19 - 3.34 Å are present.[19] Conversely, in the MEP map of MeImHS·I_2 the highest value (deep blue) (Fig. 7) is located over the NH hydrogen. Other extended blue region overlaps the CH-CH-N-CH_3 hydrogens. In the three adducts, the orange-red colouring associated with the sulphur atom is indicative both of its electron-donor capacity towards metal ions, and its ability to behave as hydrogen bond acceptor.[10b]

When an I_2 molecule is involved in a donor-acceptor interaction, a redistribution of electron density takes place causing an anisotropy of the molecule's electrostatic potential.[30,31] Therefore a distinct region of positive electrostatic potential is formed on the tip of the terminal iodine atom, commonly known as σ-hole,[31] and a negative region of electrostatic potential forming an "electron belt" around the iodine atom, perpendicular to the σ-hole. The electron belt electrostatic potential values of energy for iodine atoms I1 and I2 in the adduct Me_2ImS·I_2(α) [-100 and -120 kJ/mol] compared to those in MeImHS·I_2

[-92 and -102 kJ/mol] (Fig. 6 and Fig. 7, respectively) show differences due to the methylation of both nitrogen atoms in Me_2ImS that increases the negative charge on the sulphur atom, thus leading to an increase in the donor capacity of the molecule compared to MeImHS.

The σ-hole electrostatic potential value of energy on I2 results slightly higher in the adduct $Me_2ImS{\cdot}I_2(\alpha)$ than $MeImHS{\cdot}I_2$ [+18 and +20 kJ/mol, respectively]. The iodine atoms in the $[(Me_2ImS){\cdot}(I_2){\cdot}(I_2)]$ fragment of compound **1** show both the orange-red regions of electronic belt on iodine I(2), I(3), and I4 and the clearly visible σ-hole yellow-green regions on both iodine I2, and I4 (Fig. 5). Although each of the four iodine atoms in $[(Me_2ImS){\cdot}(I_2){\cdot}(I_2)]$ has a negative value of electron belt electrostatic potential, only iodine I4 has an σ-hole electrostatic potential favorable to the formation of interactions with donor species. This observation is reflected in the behavior of I(4) in the crystal packing of compound **1** to bind the bridging diiodine I(5)-I(5)[a] molecule and to establish an interaction with iodine I(4) from an adjacent molecule.

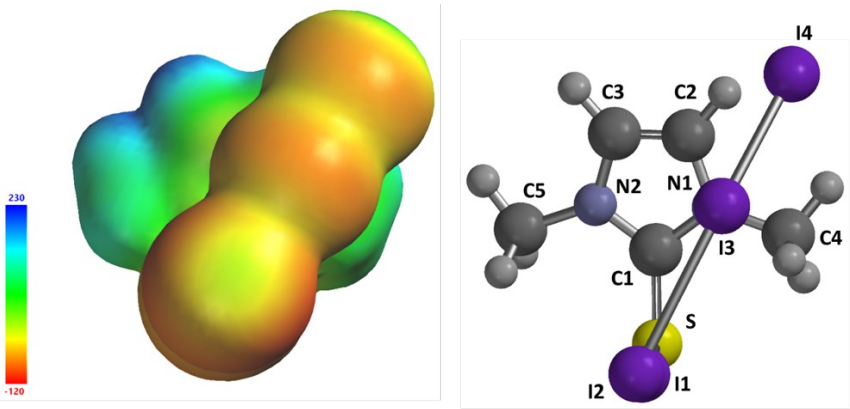

Fig. 5 MEP map on the 0.002 a.u. isodensity surface of the fragment $[(Me_2ImS){\cdot}(I_2){\cdot}(I_2)]$ of compound **1**. Colour scale of -120 kJ/mol (red) to 230 kJ/mol (blue). The electron belt electrostatic potential values on I1, I2, I3 and I4 are -91, -98, -70, and -65 kJ/mol, respectively; the σ-hole electrostatic potential values on I2 and I4 are -8 and +98 kJ/mol, respectively.

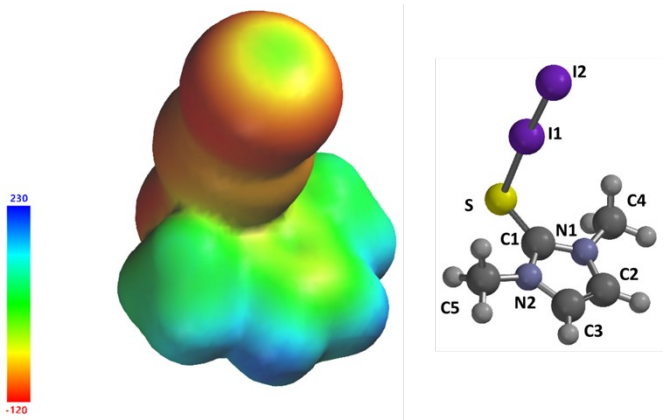

Fig. 6 MEP map on the 0.002 a.u. isodensity surface of the 1:1 C.T.-adduct $Me_2ImS{\cdot}(I_2)$ (α). Colour scale of -120 kJ/mol (red) to 230 kJ/mol (blue). The electron belt electrostatic potentials values on I1

and I2 are -100 and -120 kJ/mol, respectively; the σ-hole electrostatic potential value on I2 is +18 kJ/mol.

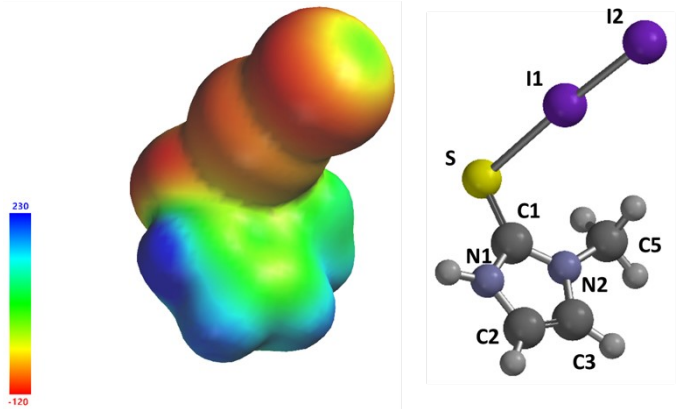

Fig. 7 MEP map on the 0.002 a.u. isodensity surface of the 1:1 C.T.-adduct MeImHS·(I_2). Colour scale of -120 kJ/mol (red) to 230 kJ/mol (blue). The electron belt electrostatic potentials values on I1 and I2 are -92 and -112 kJ/mol, respectively; the σ-hole electrostatic potential value on I2 is +20 kJ/mol.

Conclusion

The thioamide 1,3-dimethyl-imidazole-2-thione (Me_2ImS) is a simple organic molecule structurally related to the antithyroid drug methimazole. We have reported the synthesis and X-ray characterisation of the new molecular adduct [$(Me_2ImS)_2\cdot(I_2)_5$] obtained by reacting in CH_2Cl_2 solutions of I_2 and Me_2ImS in a 2:1 molar ratio. The X-ray crystal structure of the isolated poly(I_2) centrosymmetric adduct features a chain of five diiodine molecules interacting head-to-tail and with one Me_2ImS unit at each end of the poly(I_2) chain. [$(Me_2ImS)_2\cdot(I_2)_5$] represents a rare example of a neutral extended poly(I_2) arrangement held up by soft-soft $I_2\cdots I_2$ interaction at the Me_2ImS template. The *S*-bonding of Me_2ImS to I_2 is described as donor-acceptor in which I_2 acts as acceptor through the σ*(I-I) orbital resulting in an electronic charge transfer of 0.36 |e| from the thioamide moiety. The correlated bond distances *d*(S-I(1)) and *d*(I(1)-I(2)) are indicative of a strong interaction. Based on the S-I and I-I bond distances and the calculated values of the electronic charge densities, it is reasonable to represent the compound as an extended polarised system:

$$[(Me_2ImS)\text{-}I(1)]^{\delta+}\cdots I(2)^{\delta-}\cdots I(3)\text{-}I(4)^{\delta-}\cdots(I(5)\text{-}I(5)^{a})\cdots I^{\delta-}\text{-}I\cdots I^{\delta-}\cdots[(I\text{-}(Me_2ImS)]^{\delta+}$$

MEP maps of the three adducts $Me_2ImS\cdot I_2(\alpha)$, $Me_2ImS\cdot I_2\cdot I_2$, and MeImHS·$I_2$ are displayed, showing the electrostatic potential on the molecules and clearly identifying the areas of charge increment (electron belt) and depletion (σ-hole) and therefore the directionality of noncovalent interactions. Similar to the drug methimazole, Me_2ImS has a high capacity to form stable solid adducts with I_2. However, for Me_2ImS it was possible to isolate a diiodine rich adduct with a Me_2ImS:I_2 molar ratio of 1:2.5 as compared to the 1:1 molar ratio for the MeImHS·I_2 adduct. The presence of two *N*-Me in

Me_2ImS does not favor, as in the case of methimazole, oxidation-reduction processes that leads to the formation of ionic organic species (*e.g.* dication methimazole-disulfide) and polyiodides.[8] It could be assumed that Me_2ImS, if used as an antithyroid drug, may have fewer side effects than methimazole due to the NH hydrogen present in the latter species being susceptible to attack by nucleophilic species such as glutathione and DNA nucleobases. This leads to a decrease in both glutathione, and oxidation of the nucleobases causing cellular toxicity due to oxidative stress and DNA damage, respectively.[32]

Experimental

All reactants and solvents were used as purchased from Aldrich. Elemental analyses were obtained using a Perkin Elmer Series II - 2400. The 1,3-dimethyl-imidazole-2-thione (Me_2ImS) was synthesized according to Ansell[33].

Synthesis of $(Me_2ImS)_2\cdot(I_2)_5]$. Refrigerated solutions (T = 10 °C) of I_2 (100 mg, 0.394 mmol, 20 mL and Me_2ImS (37.8 mg, 0.394 mmol, 20 mL) in HPLC-grade CH_2Cl_2 were simultaneously added, 1mL at a time, over a period of 20 minutes to 10 mL of CH_2Cl_2 to give a dark reddish solution. Then the solution was left to stand for 24 hours at T = 10°C and filtered through a glass filter G4. Another equivalent of iodine (100 mg, 0.394 mmol)) in 20 mL of CH_2Cl_2 and T = 10 °C was added drop by drop over a period of 20 minutes to the solution. Slow concentration of the solution at T = 10 °C up to about 15 mL and subsequent filtration before cooling at 5 °C for about 7 days gave small dark-red crystals which were washed with cold n-hexane, and stored at low temperature. Yield: 0.095 g, 40 % referred to I_2; $C_5H_8I_5N_2S_1$ M (762.69 g/mol): calcd % C 7.87, H 1.06, N 3.67. Found: C 8.0, H 1.2, N 3.8.

Raman spectroscopy

Raman spectroscopy experiments were performed in back-scattered geometry with a non-confocal micro-Raman OEM system. The emission at 785 nm from a fiber-coupled laser diode (BWTEK BRM-785) was focused onto the samples by means of a 10 X microscope objective (laser spot diameter on the sample ~ 200 micron). Raman signals were recorded by a fiber-coupled grating spectrometer coupled with a Peltier cooled CCD (BWTEK BTC667N-785S) with spectral resolution better then 5 cm^{-1}. The Rayleigh scattering was rejected by means of an edge-filter cutting at nearly 65 cm^{-1}. The laser power was kept below 3 mW to avoid sample melting.

X-ray structure determination

A summary of the crystal data and refinement details for compound **(1)** is given in Table S1 in the ESI. Intensity data were collected at T = 293 K on a Enraf Nonius CAD4 diffractometer using graphite-monochromatized Mo-Kα radiation (λ = 0.71073 Å). Datasets were corrected for Lorentz-polarization

effects and for absorption (Psi-scan semiempirical correction) [34]. The structure was solved by direct methods (SIR-97) [35] and completed by iterative cycles of full-matrix least squares refinement on F_o^2 and ΔF synthesis using the *SHELXL*-2017 program [36] (WinGX suite) [37]. Hydrogen atoms, located on the ΔF maps, were also included in the structural model. Selected interatomic distances and angles for compound **1** are reported in Table S2 in the ESI. Crystallographic data for compound **1** have been deposited with the Cambridge Crystallographic Data Centre as supplementary publication no. CCDC 2133501. These data can be obtained free of charge via www.ccdc.cam.ac.uk/conts/retrieving.html (or from CCDC, 12 Union Road, Cambridge CB2 1EZ, UK; fax: +44 1223 336033; e-mail: deposit@ccdc.cam.ac.uk.

Computational studies.

Geometry optimization of $(Me_2ImS)\cdot(I_2)\cdot(I_2)$, $Me_2ImS\cdot I_2(\alpha)$ and $MeImHS\cdot I_2$ was performed on an Intel-i7 based system using Spartan'18 (Wavefunction Inc.) by DFT calculations using ωB97X-D as the density functional, including a Grimme's dispersion correction term,[38] and 6-31G* as the basis set. Relativistic Effective Core Potentials were adopted for the heavier atomic species. IR frequency computations were carried out to verify the nature of the minima at each optimization step, by assessing the absence of calculated negative frequencies. Heat of formation, electron density surface, atomic, electrostatic,[39] natural,[40] Mulliken charges,[41] and HOMO and LUMO energies were also calculated.

Conflicts of interest

There are no conflict to declare

Acknowledgements

We would like to thank Regione Autonoma della Sardegna for financial support. We thank CeSAR (Centro Servizi d'Ateneo per la Ricerca) of the University of Cagliari, Italy, for providing Raman facilities.

Notes and references

1. V. Lippolis and F. Isaia, Charge-Transfer (C.-T.) adducts and Related Compounds, in Handbook of Chalcogen Chemistry: New Perspectives in Sulfur, Selenium and Tellurium, ed. F. Devillanova and W.-W. du Mont, 2nd edn, **2013**, ch. 8.2, vol. 1, pp. 448–472.
2. (*a*) Aakeröy, C. B.; Wijethunga, T. K.; Desper, *J. Mol. Struct.*, **2014**, 1072 (1), 20–27; (*b*) M. Erdélyi, *Biochemistry*, **2017**, 2759-2762; (*c*) P. D. Boyle, S.M. Godfrey, *Coord. Chem. Rev.*, **2001**, 223, 265-299, and references therein.

3. W.-W. du Mont, *Main Group Chem. News*, **1994**, 2, 18-26.
4. N. Khun, T. Kratz, G. Henkel, *Z. Naturforsch. B, Chem. Sci.*, **1996**, 51, 295-297.
5. (*a*) M. C. Aragoni, M. Arca, A. J. Blake, F.A. Devillanova, W.-W. du Mont, A. Garau, F. Isaia, V. Lippolis, G. Verani, C. Wilson, *Angew. Chem.*, *Int. Ed.*, **2001**, 40, 4229-4232; (*b*) M. Arca, F. Demartin, F. A. Devillanova, A. Garau, F. Isaia, V. Lippolis, G. Verani, *J. Chem. Soc. Dalton Trans*., **1999**, 3069-3073; (*c*) F. Demartin, P. Deplano, F. A. Devillanova, F. Isaia, V.Lippolis, G. Verani, *Inorg. Chem.,* **1993**, 32, 3694-3699
6. N. Khun, R. Fawzi, T. Kratz, M. Steimann, G. Henkel, *Phosphorus, Sulfur and Silicon*, **1996**, 112, 225-233.
7. N. Khun, H. Bohnen, G. Henkel, *Z. Naturforsch. B, Chem. Sci.*, **1994**, 49, 1473-1480.
8. M. C. Aragoni, M. Arca, F. Demartin, F. A. Devillanova, A. Garau, F. Isaia, V. Lippolis, G. Verani, *J. Am. Chem. Soc.*, **2002**, 124, 4538-4539.
9. D. W. Allen, R. Berridge, N. Bricklebank, S. D. Forder, F. Palacio, S. J. Coles, M. B. Hursthouse, P.J. Skabara, *Inorg. Chem.*, **2003**, 42, 3975-3977.
10. (*a*) F. Isaia, M. C. Aragoni, M. Arca, C. Caltagirone, C. Castellano, F. Demartin, A. Garau, V. Lippolis, T. Pivetta, *Green Chem*., **2017**, 19, 4591-4599; (*b*) metimaz- Hg F. Isaia, M. C. Aragoni, M. Arca, C. Caltagirone, C. Castellano, F. Demartin, A. Garau, V. Lippolis, *Dalton Trans*., **2011**, 40, 4505-4513.
11. F. Isaia, M. C. Aragoni, M. Arca, C. Caltagirone, C. Castellano, F. Demartin, A. Garau, V. Lippolis, T. Pivetta, *New. J. Chem*., **2020**, 44, 2652-26560.
12. Methimazole is an antithyroid drug that has been used in medical practice since 1950. By preventing iodine and thyroperoxidase enzyme from their interaction with thyroglobulin to form thyroid hormone thyroxine (T4) and triiododothyronine (T3), methimazole decreases thyroid hormone production. (*a*) E. B. Burch, D. S. Cooper, *European Journal of Endocrinology*, **2018**, 179, R261-R274; (*b*) D.S. Cooper, *N. Engl. J. Med.,* **2005**, 352, 905-917.
13. (*a*) A. Suszka, *J. Chem. Soc., Perkin Trans., 2*, **1985**, 531-534; (*b*) C. Laurence, M. J. El Ghomari, J.-Y. Le Questel, M. Berthelot, R. Mokhlisse, *J. Chem. Soc., Perkin Trans., 2*, **1998**, 1545-1551; (*c*) C. Ouvrard, J.-Y. Le Questel, M. Berthelot, C. Laurence, *Acta Cryst*., **2003**, B59, 512-526.
14. W. T. Pennington, T. W. Hanks and H. D. Arman, in Halogen Bonding: Fundamentals and Applications, ed. P. Metrangolo and G. Resnati, Spinger-Verlag, Berlin, 2008, pp. 65–104, and references cited therein;
15. The adduct bond formation originates from interaction between the I_2 σ* MO (acceptor) and the nonbonding orbital of sulphur atom (*n*) of DS (donor). As a result, the σ* MO will be raised

while the energy of the *n* MO of the donor will be lowered. K. F. Purcell, J. C. Kotz, *in Inorganic Chemistry,* W. B. Saunders Company, **1977**, chapter 5, pg 210-211.

16. (*a*) M. Arca, M. C. Aragoni, F. A. Devillanova, A. Garau, F. Isaia, V. Lippolis, A. Mancini, G. Verani, *Bioinorganic Chemistry and Applications*, Volume 2006, Article ID 58937, Pages 1-12; (*b*) F. Cristiani, F. Demartin, F.A. Devillanova, F. Isaia, V. Lippolis, G. Verani, *Inorg. Chem.*, **1994**, 33, 6315-6324; (*c*) M. Ara, F. Demartin, F.A. Devillanova, A. Garau, F. Isaia, V. Lippolis, G. Verani, *J. Chem. Soc., Dalton Trans.*, **1999**, 3069-3073; (*d*) F.H. Herbstein, W. Schwotzer, *J. Am. Chem. Soc.*, **1984**, 106, 2367-2373; (*e*) W.W. Schweikert, E.A. Meyers, *J. Phys. Chem.*, **1968**, 72, 1561-1565.
17. M. C. Aragoni, M. Arca, F. Demartin, F. A. Devillanova, A. Garau, F. Isaia, V. Lippolis, G. Verani. *J. Am. Chem. Soc.,* **2002**, 124, 4538-4539.
18. F. Isaia, M. C. Aragoni, M. Arca, F. Demartin, F. A. Devillanova, G. Floris, A. Garau, M. B. Hursthouse, V. Lippolis, R. Medda, G. Verani, *J. Med. Chem.,* **2008**, 51, 4050-4053.
19. F. Freeman, J. W. Ziller, H. N. Po, M. C. Keindl, *J. Am. Chem. Soc.,* **1988**, 110, 2586-2591.
20. M. Savastano, *Dalton Trans*., **2021**, 1142-1165, and references therein.
21. (*a*) A. Bondi, *J. Phys. Chem*., **1964**, 68, 441-452; (*b*) Y. Chernishov, I. V. Ananyev, E. A. Pidko, *ChemPhysChem*, **2020**, 21, 370-376.
22. F. von Bolhuis, P. B. Koster, T. Migchelsen, *Acta Crystallogr*., **1967**, 23, 90-91.
23. The bond order *n*(I-I) can be evaluated according to the empirical function proposed by Pauling and adapted by Burgi: $n(\text{I-I}) = \exp[d_0(\text{I-I}) - d(\text{I-I})/b]$ (where d_0 is the I-I bond distance for I_2(g) and *b* is an empirical constant with a value of 0.85). (*a*) L. Pauling, *J. Am. Chem. Soc*., **1947**, 69, 542-553; (*b*) H. B. Burgi, J. D. Dunitz, *J. Am Chem. Soc.,***1987**, 109, 2924-2926.
24. F. H Allen, D. G. Watson, L. Brammer, A. G. Orpen, R.Taylor (**2006**) Typical interatomic distances: organic compounds. In: Prince E. (eds) International Tables for Crystallography Volume C: Mathematical, physical and chemical tables. International Tables for Crystallography, vol C. Springer, Dordrecht. https://doi.org/10.1107/97809553602060000621
25. F. H. Herbstein, W. Schwotzer, *J. Am. Chem. Soc.,* **1984**, 106, 2367-2373.
26. M. D. Rudd, S. V. Lindeman, S. Husebye, *Acta Chem. Scan*., **1997**, 51, 689-708.
27. (*a*) A. Anderson, T. S. Sun, *Chem. Phys. Lett*., 1970, 6(6), 611-616; (*b*) P. Deplano, F. A. Devillanova, J. R. Ferraro, F. Isaia, V. Lippolis, M. L. Mercuri, *Appl. Spectrosc*., **1992**, 11, 1625-1629;
28. (*a*) T. Horibe, Y. Tsuji, K. Ishihara *ACS Catal*. **2018**, 8, 7, 6362–6366; (*b*) A. Mancini, M. C. Aragoni, A. L. Bingham, C. Castellano, S. L. C. Huth, F. Demartin, M. B. Hursthouse, F. Isaia, V. Lippolis, G. Maninchedda, A. Pintus, M. Arca, *Chem. Asian J*., **2013**, 8(12), 3071-3078; (*c*)T. Horibe, Y. Tsuji, K. Ishihara, *Org. Lett*., **2020**, 22, 12, 4888–4892.

29. (*a*) P. Politzer, J. S. Murray, Z. Peralta-Inga, *Int. J. Quantum Chem.,* **2001**, 65, 676-684.; (*b*) J. S. Murray, P. Politzer, *WIREs Comput. Mol. Sci.*, **2011**, 1, 153-163; (*c*) T. Clark, *Faraday Discuss*., **2017**, 203, 9-27.
30. G. Cavallo, P. Metrangolo, R. Milani, T. Primati, A. Primigi, G. Resnati, G. Terraneo, *Chem. Rev.,* **2016**, 116, 2478-2601.
31. M. V. Chernysheva, M. Bulatova, X. Ding, M. Haukka, *Cryst. Growth & Des*., **2020**, 20(11) 7197-7210.
32. F. Huq, *J. Pharmacol. Toxicol*., **2008**, 3(1), 11-19.
33. G. B. Ansell, D. M. Forkey, D. W. Moore, *J. Chem. Soc., Chem. Commun.*, **1970**, 56-57.
34. A. C. T. North, D. C Phillips, F. S. Mathews, *Acta Crystallogr.* Sect. A **1968**, 24, 351-359**.**
35. A. Altomare, M. C. Burla, M. Camalli, G. L. Cascarano, C. Giacovazzo, A. Guagliardi, A. G. G. Moliterni, G. Polidori, R. Spagna, *J. Appl. Cryst.,* **1999**, 32, 115-119.
36. G. M. Sheldrick, Crystal structure refinement with SHELXL. *Acta Crystallogr., Sect. C*: Struct, Chem., **2015**, *71*, 3–84)
37. L. J. Farrugia, *J. Appl. Crystallogr.,* **1999**, 32, 837-838.
38. S. Grimme, J. Antony, S. Ehrlich, H. Krieg, *J. Chem. Phys.,* **2010**, 132, 154104
39. L. E. Chirlian, M. M. Francl, *J. Comput. Chem*., **1987**, 8, 894-905; (b) C. M. Breneman, K. B. Wiberg, *J. Compt. Chem*., **1990**, 11, 361-373; (b) M. Breneman and K. B. Wiberg , *J. Comput. Chem.,* **1990**, 11, 361-373.
40. A. E. Reed, R. B. Weinstock, F. Weinhold, *J. Chem. Phys*., **1985**, 83, 735-746.
41. (a) R. S. Mulliken, J. *Chem. Phys.,* **1955**, 23, 1833-1840; (b) R. S. Mulliken, J. *Chem. Phys.,* **1955**, 23, 2338-2342.